

Theory of angle-resolved photoemission from the bulk bands of solids. II. Application to Ag(111)

D. Liebowitz and N. J. Shevchik

Department of Physics, State University of New York, Stony Brook, New York 11794

(Received 23 February 1978)

It is shown that the angle-resolved photoemission spectra computed from the theory developed in Paper I, which is based upon a free-electron final state, atomic dipole selection rules, and the band structure of the bulk, are in good agreement with the experimental spectra from a Ag(111) surface for $h\nu = 16.9, 21.2, 26.9,$ and 40.8 eV. There is some sporadic indication that multiple-scattering effects are present in the spectra obtained for $h\nu = 40.8$ eV. We conclude that there are no significant modifications of the bulk bands at the surface, nor any conclusive signs of surface states.

I. INTRODUCTION

In several earlier papers, it has been shown that the simple free-electron-final-state (FEFS) model serves to locate the positions of the peaks in the angle-resolved photoemission spectra of the noble metals.¹⁻⁶ We have proposed in paper I,⁷ a one-step model based upon the FEFS model for explaining both the positions and intensities of the peaks in the angle-resolved photoemission spectra of solids. In this model, atomic-dipole selection rules dominate the behavior of the optical ionization process, but the plane waves govern the energy dispersion, the transport, and the escape processes of the photoelectron. The initial electron states are assumed to be those of the bulk; the influence of the surface in mixing the bulk states and in forming surface states is completely ignored. A preliminary report of the success of this model for Cu has appeared recently.⁶ However, it is not clear whether this model ought to apply to Ag where the stronger atomic potential can make multiple-scattering effects important.

In this paper the computed predictions of our model using a tight-binding initial-state band structure are shown to be in good general agreement with extensive angle-resolved photoemission data from a Ag(111) surface.

II. APPLICATION OF THE MODEL TO Ag(111)

A. Initial-state energy bands

The initial-state energies and eigenfunctions were computed in a tight-binding two-centered approximation⁸ using the five $4d$ orbitals and a $6s$ orbital. We chose the spin-orbit interaction to yield a splitting of 0.6 eV between $J = \frac{5}{2}$ and $\frac{3}{2}$ d orbitals. The interaction parameters were adjusted to obtain as good agreement as possible with the results of Smith⁹ and Christensen.¹⁰ The

parameters used were

$$ss = -0.56 \text{ eV}, \quad sd = -0.5 \text{ eV},$$

$$dd\sigma = -0.45 \text{ eV}, \quad dd\pi = +0.20 \text{ eV},$$

$$dd\delta = -0.02 \text{ eV}, \quad E_d = -5.4 \text{ eV}, \quad E_s = -0.8 \text{ eV}.$$

The small discrepancies (0.3 eV) between our results and those of Smith⁹ and Christensen¹⁰ were probably due to the neglect of the higher-lying plane-wave states above the Fermi energy.

B. Computation of the spectra

For a smooth surface, the component of the wave vector of the photoelectron parallel to the surface is^{11,12}

$$k_{\parallel} = k_0 \sin \theta, \quad (1)$$

where k_0 is the magnitude of the momentum in free space and θ is the polar angle of emission. The photoelectron inside the solid must have exactly the same component of momentum parallel to the surface to ensure that the wave function matches at the solid-vacuum interface. The component of momentum inside of the solid perpendicular to the surface is calculated using⁷⁻⁹

$$k_{\perp} = (2m^*E/\hbar^2 - k_{\parallel}^2)^{1/2}, \quad (2)$$

where E is the kinetic energy of the photoelectron in the solid measured with respect to the bottom of the s band and m^* is the effective mass of the internal photoelectron which is close to, but not necessarily equal to, the mass of the free electron.

Including the finite mean free path of the photoelectron, the intensity according to the model introduced in I is^{6,7}

$$I(E_f(\vec{k}_f)) \propto \sum_n \int |\sigma_n(\vec{k})|^2 \delta(E_f(\vec{k}_f) - E_n(\vec{k}) - \hbar\omega) \times \frac{\Gamma dk'_1}{\Gamma^2 + (k'_1 - k_1)^2}, \quad (3)$$

where $\vec{k} = \vec{k}_{\parallel} + \vec{k}_{\perp}$, $\vec{k}_f = \vec{k}_{\parallel} + \vec{k}_{\perp}$ and $\Gamma = 1/l \cos \theta$, l is the mean free path of the photoelectron and θ is the angle between the surface normal and the direction of propagation of the photoelectron inside of the solid. The Lorentzian factor in Eq. (1) accounts for the weakening of the conservation of the component of the photoelectron momentum perpendicular to the surface due to the finite mean free path of the photoelectron.^{11,12} The energy dispersion of the initial state $E_n(\vec{k})$ we take to be periodic in \vec{k} space, while the energy dispersion of the final state is given by that of the free electron. The atomiclike cross sections are contained in the term $|\sigma_n(\vec{k})|^2$. The summation index n extends over the filled bands. For the unpolarized light used in our experiments on silver, we find using the formalism in I that the angular behavior and orbital dependence of the atomic cross section from initial-state d and s orbitals is^{6,7}

$$|\sigma_n(\vec{k})|^2 \propto \{[\lambda C_{d2}^n(\vec{k}) + \lambda_s C_s^n(\vec{k})] \sin \beta + C_{xy}^n(\vec{k}) \cos \beta\}^2 + [C_{xz}^n(\vec{k})]^2, \quad (4)$$

where β is the angle between \vec{k}_f and the Poynting vector. We have not taken into account the modification of the electric field due to the dielectric response of Ag and have assumed it to have the same direction as in free space. The d orbital coefficients of the initial states C_{d2} , C_{xy} , C_{xz} are with respect to a coordinate system where the z axis is along the momentum \vec{k}_f and the y axis is in the plane containing \vec{k} and the Poynting vector of the incident light. The quantity λ is the ratio of the $m=0$ to $|m|=1$ photoionization matrix element which has the values for the free atom of $2/\sqrt{3}$ and $-\sqrt{3}$ for $d \rightarrow p$ and $d \rightarrow f$ transitions, respectively.¹³ For low photon energies ($h\nu \lesssim 20$ eV) the $d \rightarrow p$ channel dominates while for higher energies ($40 \text{ eV} \leq h\nu$) the f channel dominates.¹⁴ λ was set at 0.6 for NeI, 0.87 for HeI, and 1.4 for HeII to simulate the change in the optical transition from $d \rightarrow p$ to $d \rightarrow f$ character. In the energy region where both p and f final states contribute to the matrix element, the value of λ can assume any complex value depending upon the relative magnitude and phase of the p and f contributions to the matrix element.¹³ In the computations, Γ at normal emission was set at 0.07 \AA^{-1} for NeI and 0.31 \AA^{-1} for HeI and HeII. The s cross section was taken to be 0 for HeI and HeII since no strong s -band structure was observed in the spectra obtained for these energies. For NeI, a value of $\lambda_s = 1.0$ was usually used to duplicate the features associated with the s -like band. The computed spectra were broadened by 0.3 eV to simulate lifetime effects and instrumental resolution.

Since we were interested in describing only the changes in the shape of the spectra with angle of emission, rather than the photon energy dependence, it was never necessary in the computation to calculate an explicit final electron state. The spectra were computed in about 15 min. on a PDP-11 minicomputer.

III. RESULTS AND DISCUSSION

The experimental details and some of the spectra presented here have been presented elsewhere⁵ and therefore the present discussion will focus upon the theoretical spectra and their relationship to the experimental results.

A. Normal emission

A comparison of the theoretical calculations and the experimental results of Roloff and Neddermeyer¹⁵ for $h\nu = 16.9$ and 21.2 eV for electrons emitted normal to the (110) surface is presented in Fig. 1. The strength of the peak at ~ 7 -eV binding energy is overestimated in the calculated spectra. The values of the parameters used in these spectra gave good agreement for emission from the (111) face, and therefore we believe that the discrepancy is related to our neglect of the influence of the dielectric response in reducing the strength of the component of the electric field normal to the surface.^{16,17} Otherwise, it is noteworthy that our calculated spectra from the (110) face show agreement with experiment, since previous interpretations in terms of the bulk band structure were not successful.¹⁸ The band structure for the Σ axis reveals that if transitions to other than the single free-electron final-state band were contributing to the spectrum, pronounced contributions from near the Γ point should occur at the center of the spectra, such as have been reported earlier.¹⁸ Small contributions in the middle of the d bands are present for HeI. Our calculations, for a larger uncertainty in k_{\perp} , begin to

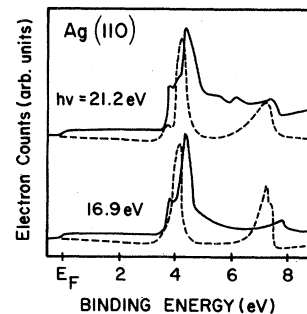


FIG. 1. NeI and HeI experimental (solid line) and calculated (dashed line) photoemission spectra for normal emission from Ag(110).

show these contributions as the Lorentzian factor in Eq. (3) extends over states near the Γ point. For NeI, the contributions in the middle of the two peaks are virtually nonexistent. Thus, transitions to final state bands other than the free-electron band propagating in the $[110]$ direction are not observed even though the probability of excitation into these bands is similar to that of the single band propagating along the axis of emission. The free-electron final-state model passes a severe test in the $[110]$ direction.

Note that the positions of the peaks in the calculated spectra show no significant movement between 16.9 and 21.2 eV, in agreement with experiment. Usually, it has been assumed that the lack of movement of peaks with photon energy indicates the breakdown of \vec{k} conservation.¹² However, according to our model such a behavior is expected for two reasons. First, the initial-state bands are flat in the region contributing to emission. Second, although the details of the other final-state band structure change with photon energy, only the one state that propagates in the direction of emission contributes to the spectra. Increasing the energy by a few electron volts changes the momentum of the relevant final state by only $\sim \frac{1}{10}$ the width of the Brillouin zone.

The theoretical spectra of electrons emitted normally from the (111) surface for $h\nu = 16.9, 21.2, 26.9,$ and 40.8 eV are in good agreement with experimental results (see Fig. 2). Earlier we suggested that the increasing strength of the peak

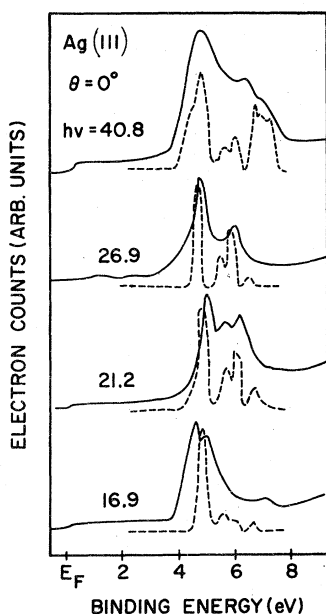


FIG. 2. Normal-emission photoemission spectra from Ag(111). The solid line is the experiment and the dashed line is the theory.

near ~ 6 eV binding energy with photon energy was an indication that the final state was being hybridized by the crystal potential, invalidating the simple atomic-dipole selection rules.¹⁹ Our assumption that the deeper bands in Ag were derived from orbitals primarily with angular momentum quantum number $|m| = 2$ was correct, but as the present calculations show, these bands have a large $|m| = 1$ and $m = 0$ character near the Γ point. The movement of k_{\perp} closer to the Γ point for $h\nu$ changing from 16.9 to 26.9 eV accounts for the increase in the strength of the peak near 6-eV binding energy. For $h\nu = 40.8$ eV, the region in \vec{k} space contributing to direct transitions is nearly the same as for $h\nu = 16.9$ eV. However, the larger 6.5-eV peak for $h\nu = 40.8$ eV is due to the fact that the photoionization cross sections for the $m = 0$ initial states triples as the $d \rightarrow f$ channel opens up. The middle peak at 5.8-eV binding according to the calculation still has a large $|m| = 2$ character, accounting for its weak intensity. The observed high intensity of this peak is an indication that the final state is strongly hybridized, but it is by no means conclusive.¹⁹ It has been shown elsewhere that the final electron state in Cu remains unhybridized for $h\nu$ extending to 150 eV.²⁰ However, hybridization of the final state in Ag could occur since it has a stronger atomic potential than Cu. The spectra obtained for non-normal emission (see below) indicate that multiple-scattering effects are of some importance for $h\nu = 40$ eV.

B. Non-normal emission

The experimental and theoretical spectra for non-normal emission for NeI and HeI are displayed in Figs. 3–8. For HeI and NeI in the $\Gamma L K L$ and $\Gamma L U X$ directions generally good agreement is obtained between theory and experiment, while in the $\Gamma L W$ direction there are significant discrepancies. We list the major features which appear in both experiment and theory.

(i) In the $\Gamma L K L$ direction for both NeI and HeI (Figs. 3 and 4) the spectra away from normal emission consist of two peaks, one at the top and the other at the bottom of the d bands. The peak at the top of the d bands is much more pronounced than the peak at the bottom.

(ii) In the $\Gamma L U X$ direction for NeI (Fig. 5) a three-peak structure is observed. The theory explains the peak heights reasonably well, and it accounts for the peak occurring between E_f and 4-eV binding energy. The error in the predicted position of the peak near E_f for NeI is attributed to the inability of our tight-binding model to describe the s -like band with accuracy.

(iii) In the $\Gamma L U X$ direction for HeI (Fig. 6) for

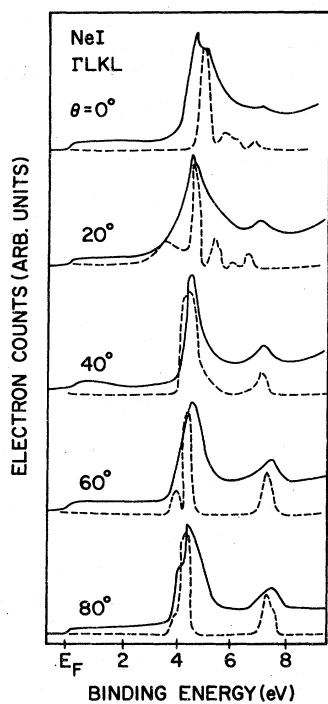


FIG. 3. Calculated (dashed line) and experimental (solid line) photoemission spectra from the ΓLKL plane for NeI ($h\nu = 16.9$ eV).

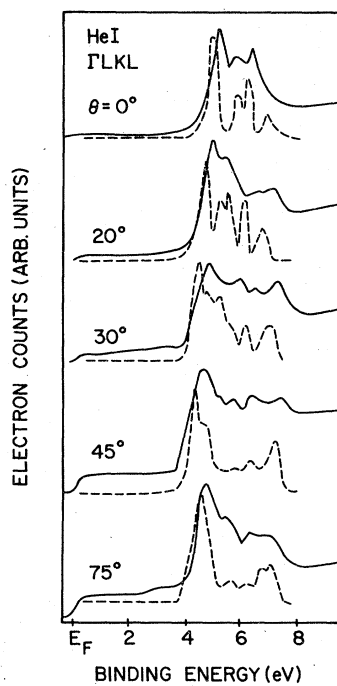


FIG. 4. Calculated (dashed line) and experimental (solid line) photoemission spectra from the ΓLKL plane for HeI ($h\nu = 21.2$ eV).

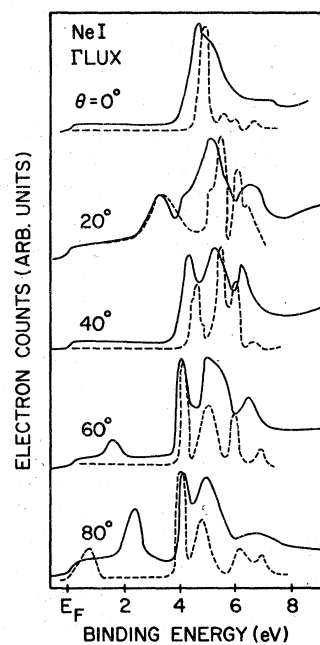


FIG. 5. Calculated (dashed line) and experimental (solid line) photoemission spectra from the ΓLUX plane for NeI ($h\nu = 16.9$ eV).

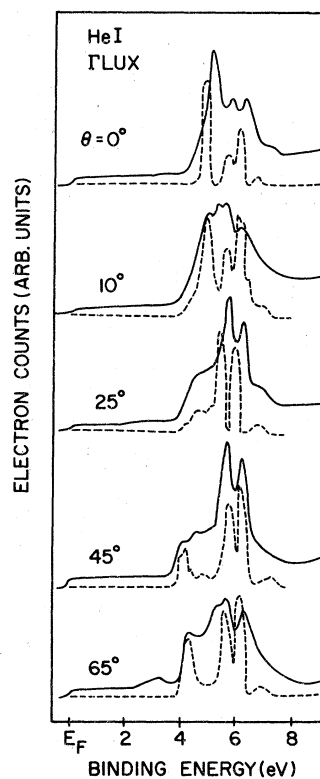


FIG. 6. Calculated (dashed line) and experimental (solid line) photoemission spectra from the ΓLUX plane for HeI ($h\nu = 16.9$ eV).

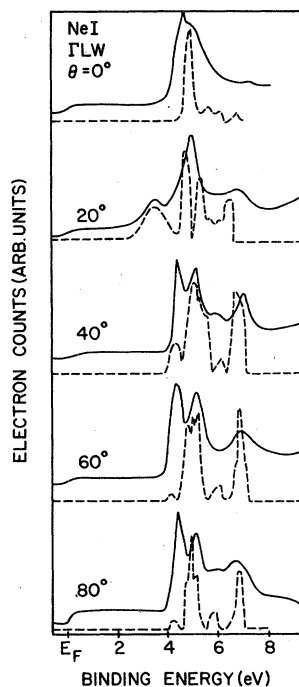


FIG. 7. Calculated (dashed line) and experimental (solid line) photoemission spectra from the ΓLW plane for Ne I ($h\nu = 16.9$ eV).

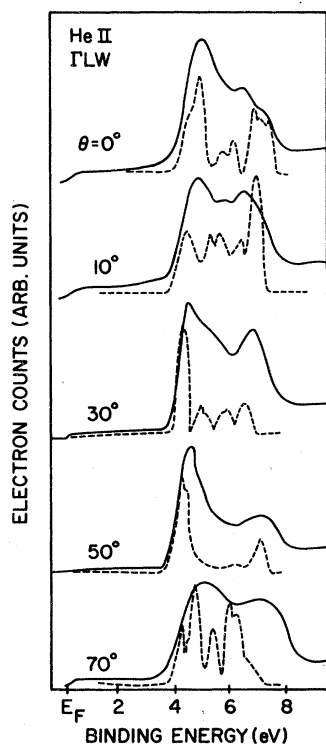


FIG. 8. Calculated (dashed line) and experimental (solid line) photoemission spectra from the ΓLW plane for He II ($h\nu = 40.8$ eV).

$\theta = 40^\circ$ and 60° , two sharp, closely spaced peaks occur in the middle d bands.

(iv) In the ΓLW direction for Ne I (Fig. 7) the experimental spectrum is characterized by two pronounced peaks at -4.1 and -5 eV, a weak peak at -5.9 eV, and a pronounced peak at -7 eV. In the calculated spectra for this direction the peak positions are approximately correct, and the intensities show agreement except for the faintness of the peak at -4.1 eV. There is very little $m = 0$ or $|m| = 1$ component along \vec{k}_z for this peak, but there is a sizable $|m| = 2$ component.

For the spectra mentioned, the peak positions never disagree by more than 0.4 eV (with the exception of some very faint structure). Many features, such as the two peaks in the Ne I spectra in the ΓLKL direction, are described more closely by the theory. The calculated structure seems somewhat too close together in the ΓLUX direction for Ne I and rigidly displaced at 0.3- or 0.4-eV decreased binding energy in the ΓLKL direction for He I.

The calculated spectra for Ne I in the ΓLUX direction were obtained by reducing the value of k_z to an amount 10% less than given by Eq. (2). The other scans were not sensitive to such adjustments in k_z ; thus it is not clear whether this phenomenon is restricted to this particular azimuthal angle alone. However, a similar adjustment was needed to explain the experimental spectra of Cu.⁶ It is possible that the final-state electron for this particular energy and direction is being perturbed away from the free-electron energy dispersion. However, if this were so, we would not expect our model for the cross sections to do so well in describing the spectra. We admit to not understanding why such a shift is needed.

The agreement between theory and experiment for $h\nu = 40.8$ eV (see Fig. 8) is not as good as for the lower photon energies. The computed spectra for $\theta = 70^\circ$ are in poor agreement with experiment while the spectra for $\theta = 50^\circ$ is in good agreement. We cannot attribute the disagreement to the somewhat worse energy (0.3 eV) and \vec{k} -space resolution for these spectra. For the larger photon energies, the \vec{k} vector is scanning as θ increases through larger regions of the Brillouin zone than for the smaller photon energies, and thus, the spectra become more sensitive to the parameters in Eqs. (2) and (3). Also for the larger final-state wave vectors, the breakdown of \vec{k} conservation due to scattering of the photoelectron by phonons and disorder becomes increasingly important, possibly destroying any relationship between the present theory and experiment.²¹

As mentioned earlier, multiple scattering²² of

the photoelectron might be accounting for the sporadic performance of the model for $h\nu = 40.8$ eV. When the pseudopotential is small, the effects of multiple scattering become important only for regions in the Brillouin zone for which the plane wave that contributes in our model becomes degenerate with plane waves propagating in other directions. Otherwise, the multiple scattering is small and our model gives results in good agreement with experiment. The fact that the $d \rightarrow f$ photoionization channel is opening up for this photon energy also suggests that f partial-wave scattering is becoming intense.

The theory has demonstrated that it can also account for the peak shapes as well as position and intensity. Narrow peaks occur when the corresponding band has a weak dispersion with k_{\perp} at the k points sampled, while broad peaks occur when the corresponding band has a large dispersion with respect to k_{\perp} . For both calculation and experiment the middle peak for Ne I spectra in the ΓLUX direction at 60° and 80° is broad, while the leading peak is narrow. For $\theta = 40^{\circ}$, however, the experiment shows the middle peak to be broad yet the calculation shows this peak to be hardly any broader than the other two peaks. For $\theta = 20^{\circ}$, the back $s-p$ structure near -3 eV and a lower peak composed of s and d bands are broad in agreement with experiment. The two pronounced peaks for He I in the ΓLUX direction are correctly predicted to be sharp, but the shoulder observed at about -4.2 eV is predicted to be a peak for $\theta = 45^{\circ}$. This is not improved by shifting k_{\perp} for a fixed k_{\parallel} . The possible sources of disagreement in the widths of the peaks are (a) a failure of our tight-binding scheme to describe the curvature of the energy bands in the direction perpendicular to the surface; (b) a lifetime broadening which varies with the orbital nature of the band; (c) contributions from surface states.

C. Comparison with plane-wave and constant matrix elements

The agreement between experiment and our theory is generally good. However, a question arises as to how well the present theory compares to other theories and models. We have ruled out the one dimensional density of states model²³ by showing that the spectra from the ΓLKL and ΓLUK planes are very much different.⁵ It is clear that some retention of the conservation of k_{\perp} is necessary to explain the experimental results. The uncertainty in k_{\perp} that we found to be necessary to bring theory into agreement with experiment is about equal to the value expected from the length of the electronic mean free path, which is ~ 10 Å. Constant matrix elements² and those calculated

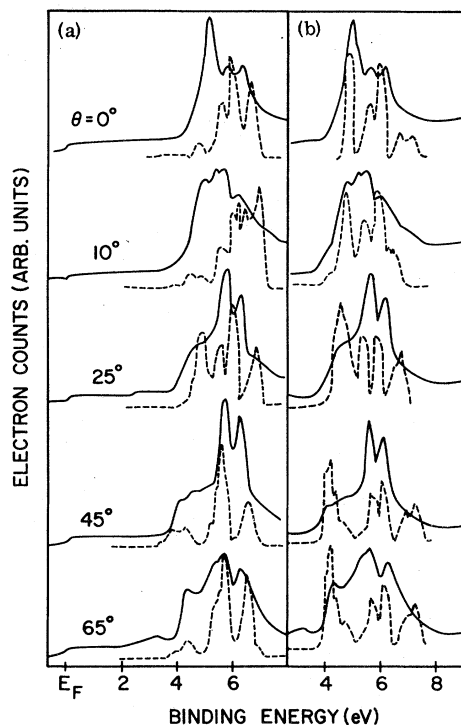


FIG. 9. Calculated photoemission spectra (dashed line) using (a) the plane-wave final state and (b) constant matrix compared with the experimental spectra (solid line) from the ΓLUX plane for He I ($h = 21.2$ eV).

from a plane-wave final state in general do a poorer job of explaining the spectra than the matrix elements based upon atomic-dipole selection rules. We show as an example, the results for the ΓLUX direction for He I. It can be seen that constant matrix elements (Fig. 9) very greatly exaggerate the intensity at the top of the d bands and, to a lesser extent, the intensity near the bottom of the d bands. The plane-wave final state shows particularly poor agreement at $\theta = 0^{\circ}$ and 10° . The agreement, however, improves as the angle of emission increases. This is to be expected since the separation of the initial-state bands according to orbital symmetry weakens for directions away from symmetry axes.

IV. CONCLUSIONS

The overall success of the theory in describing experiments indicates the following for Ag. (i) The final state is not significantly hybridized by the crystal potential. (ii) The surface is not significantly altering the electronic wave functions at the bulk; in particular, there is no obvious sign of emission from surface states.²⁴

The specific disagreements with experiment is probably attributed to a violation of one of the

above two statements. The success of our model indicates that the angle-resolved photoelectron spectra reflect the initial-state band structure in a particular region of the Brillouin zone. Although our model does not yield 100% agreement with experiment, it does open the way for a more thorough understanding of the form of the spectra expected from the bulk bands. With this done, we are now in a better position to look for effects

which are due specifically to the surface, if in fact there are any.

ACKNOWLEDGMENTS

Discussions with M. Sagurton and J. Colbert are gratefully acknowledged. This work was supported by NSF Grant No. DMR-76-12574.

-
- ¹L. F. Wagner, Z. Hussain, C. S. Fadley, and R. J. Baird, *Solid State Commun.* **21**, 453 (1977).
²L. F. Wagner, Z. Hussain, and C. S. Fadley, *Solid State Commun.* **21**, 257 (1977).
³P. M. Williams, P. Butcher, J. Wood, and K. Jacobi, *Phys. Rev. B* **14**, 3215 (1976).
⁴J. Stöhr, P. S. Wehner, R. S. Williams, G. Apai, and D. A. Shirley, *Phys. Rev. B* **17**, 587 (1978).
⁵D. Liebowitz and N. J. Shevchik, *Phys. Rev. B* **17**, 3825 (1978).
⁶D. Liebowitz, M. Sagurton, J. Colbert, and N. J. Shevchik, *Phys. Rev. Lett.* **39**, 1625 (1977).
⁷N. J. Shevchik and D. Liebowitz, *Phys. Rev. B* **18**, 1618 (1978) (preceding paper).
⁸J. C. Slater and G. F. Koster, *Phys. Rev.* **94**, 1498 (1954).
⁹N. V. Smith, *Phys. Rev. B* **9**, 1341 (1974).
¹⁰N. E. Christensen, *Phys. Status Solidi B* **54**, 551 (1972).
¹¹G. D. Mahan, *Phys. Rev. B* **2**, 4334 (1970).
¹²P. J. Feibelman and D. E. Eastman, *Phys. Rev. B* **10**, 4932 (1974).
¹³N. J. Shevchik (unpublished).
¹⁴J. W. Gadzuk, *Phys. Rev. B* **12**, 5608 (1975).
¹⁵H. F. Roloff, and P. Neddermeyer, *Solid State Commun.* **21**, 561 (1977).
¹⁶P. J. Feibelman, *Surf. Sci.* **46**, 558 (1974).
¹⁷K. L. Kliewer, *Phys. Rev. Lett.* **33**, 900 (1974).
¹⁸N. E. Christensen, in *International Symposium on Photoemission*, edited by R. F. Willis, B. Feuerbacher, B. Fitton, and C. Back Noordwijk, 1976 (European Space Agency, Paris, France, 1976).
¹⁹N. J. Shevchik and D. Liebowitz, *Phys. Rev. B* **16**, 2395 (1977).
²⁰M. Sagurton and N. J. Shevchik (unpublished).
²¹N. J. Shevchik, *Phys. Rev. B* **16**, 3428 (1977); *J. Phys. C* **10**, L555 (1977).
²²J. B. Pendry, *Surf. Sci.* **57**, 679 (1976).
²³B. Feuerbacher and N. E. Christensen, *Phys. Rev. B* **10**, 2373 (1974); T. Grandke, L. Ley, and M. Cardona, *Solid State Commun.* **23**, 897 (1977).
²⁴R. V. Kasowsky, *Phys. Rev. Lett.* **33**, 83 (1974).